EasyChair Preprint

№ 11238

Evolutionary Optimization for Tuning Barometer-Aided Inertial Navigation System Vertical Channel Mechanization

Vinícius M. G. B. Cavalcanti, Felipe O. Silva,
Álvaro H. A. Maia, Danilo A. de Lima, Alexandre C. Leite and
Jay A. Farrell

November 3, 2023

Evolutionary Optimization for Tuning Barometer-aided Inertial Navigation System Vertical Channel Mechanization ⋆

Vinícius M. G. B. Cavalcanti [*,**] **Felipe O. Silva** [**]
Álvaro H. A. Maia [**] **Danilo A. de Lima** [**] **Alexandre C. Leite** [***]
Jay A. Farrell [****]

[*] *Diretoria de Ensino, Pesquisa e Extensão, Instituto Federal de Educação, Ciência e Tecnologia Fluminense, Itaboraí, RJ, (e-mail: vinicius.cavalcanti@gsuite.iff.edu.br)*
[**] *Departamento de Automática, Universidade Federal de Lavras, MG, (e-mails: felipe.oliveira@ufla.br, alvaro.maia1@estudante.ufla.br, danilo.delima@ufla.br)*
[***] *MWF Services Ltda., Departamento de Pesquisa e Desenvolvimento, (e-mail: alexandre@mwf-services.com)*
[****] *Department of Electrical and Computer Engineering, University of California, Riverside, USA, (e-mail: farrell@ece.ucr.edu)*

Abstract: This work revisits the vertical channel mechanization problem of barometer-aided Inertial Navigation Systems (INS) and proposes a new approach to tune the gains of such a control loop. As a main contribution, it presents a performance analysis of a novel tuning method based on multi-objective optimization using evolutionary algorithms. To validate the performance of the optimized tunings, signal norms, and statistical measures are used to describe and analyze the vertical channel errors of the vertical channel control loop, which are then compared with a traditional empirical solution and with the one obtained via a recently proposed method based on Linear Quadratic Regulator (LQR). According to the experimental results, the proposed optimization technique demonstrates its reliability/robustness over multiple different data sets, as long as the data set used in the optimization procedure has dynamical characteristics that correlate to the maneuver in the evaluation data sets.

Keywords: Inertial navigation system, Barometer, Vertical channel damping, Multi-objective optimization, Genetic algorithm.

1. INTRODUCTION

Navigation is the science that deals with determining the position, velocity, and attitude of a moving body, usually a vehicle, w.r.t. a known reference (Groves, 2013). Currently, Inertial Navigation Systems (INS) and Global Navigation Satellite Systems (GNSS) are among the main technologies for vehicle navigation. They are complementary and often employed together, i.e. by means of INS/GNSS integration techniques (Farrell and Wendel, 2017), to provide accurate navigation solutions for vehicles. Nevertheless, as pointed out by Gallo and Barrientos (2022), GNSS signals are not always available. Those signals may be either accidentally corrupted due to tall buildings or terrain features (blockage or multipath propagation), or maliciously corrupted (jamming or spoofing). Under such circumstances, especially for applications with navigation over several minutes, due to the instability in the vertical channel error dynamics (Farrell, 2008, Sec. 11.5.1.1), the vertical solution of a pure INS will violate the accuracy requirements (Savage, 2000, Sec. 4.4.1.2.1). To overcome this issue, INS has historically (and additionally) been fused with barometric altimeters. In this method, the inertial vertical solution is compared with an altitude reference provided by the altimeter, and the difference is then fed back with suitable gains in a servomechanism fashion to stabilize the vertical channel.

Several authors have proposed control loops, also referred to as mechanizations, to bound INS vertical channel errors and achieve satisfactory responses in the presence of disturbances. Most of the literature on the subject relies on heuristics and classic control theory Ogata (2010) to tune such mechanizations, e.g. as in Widnall and Sinha (1980); Siouris (1993); Savage (2000); Titterton and Weston (2005); Bekir (2007); Rogers (2007). Nonetheless, recent studies on the area (Vieira et al., 2020; Silva and Vieira, 2022; Ben et al., 2023; Vieira and Silva, 2023) implies that the subject under investigation is still relevant. For instance, Vieira and Silva (2023) proposed methods

⋆ This study was financed in part by the Research Development Foundation (FUNDEP - ROTA 2030), under grant 27192.02.02/2021.01.00, in part by the Brazilian Agricultural Research Corporation (EMBRAPA), under grant 212-20/2018, in part by the Brazilian National Council for Scientific and Technological Development (CNPq), under grants 313160/2019-8 and 312194/2022-6, and in part by the Minas Gerais State Agency for Research and Development (FAPEMIG), under grants APQ-01449-17 and APQ-04659-22.

based on optimal control theory (Kirk, 2004), with the Linear Quadratic Regulator (LQR) approach being able to outperform traditional tuning methods w.r.t. the vertical channel errors' mean and standard deviation.

Control systems design has evolved since the development of the aforementioned designing tools and intelligent control techniques, enumerated e.g. in the work of de Silva (2009), have particularly attracted interest in recent years. In the broader class of evolutionary computation, Genetic Algorithms (GA) are search procedures based on natural selection whose use in control engineering has been expanded in the past decades. For a comprehensive review of such applications, the reader is referred to Goldberg (1989); Dracopoulos (1997); Wang et al. (2003); He et al. (2016); de Morais et al. (2022) and references therein.

As a main contribution, a novel tuning method based on multi-objective GA is proposed. Accordingly, the aim of this work is to further investigate modern optimization techniques to solve the INS vertical channel mechanization tuning problem. Mainly, this work is concerned with investigating the trade-off involved with the use of evolutionary algorithms to solve such a problem. This work suggests that, although the LQR solution (Vieira and Silva, 2023) performs well for generic applications, GA is able to provide tailored solutions when a specific scenario is being considered, e.g., when the user knows that the vehicle is subject to particular maneuvers. Furthermore, another contribution relates to the use of the higher degree-of-freedom architecture provided by the 3rd-order mechanization with four gains, introduced in the work of Blanchard (1971). The tuning of parameter K_4 and its impact on the mechanization performance is rarely explored or even discussed, thus the presented study attempts to fill, at least partially, this gap in the literature.

The remainder of this paper is organized as follows: Section 2 states the vertical channel problem and reviews classic empirical and optimal control tuning methods. Section 3 describes the proposed optimization approach and suggests analytical tools for comparing results. Section 4 discusses the results from experimental tests of mechanizations tuned with the proposed technique. Finally, Section 5 provides concluding remarks.

NOTATION

The following notation is adopted throughout this paper: for a given variable x, $x^{\gamma}_{\beta\alpha,Y}$ means its component Y, defined for a frame α w.r.t. the origin of frame β and resolved about frame γ, while $\delta x \triangleq \tilde{x} - \hat{x}$ means the difference, also referred as error, between a measure (raw solution) $\tilde{x}$ and its estimated value (ground-truth solution) $\hat{x}$. The closed-loop transfer function mapping w into z is denoted $T_{zw}(s)$. For a given matrix M, $\lambda_i(M)$ denotes its ith eigenvalue.

2. VERTICAL CHANNEL PROBLEM STATEMENT

2.1 Inertial solution

In pure INS, vertical acceleration $a^n_{eb,U}$ is computed as the sum of specific force measured by accelerometers in the vertical direction, gravity acceleration, and additional terms due to centrifugal and Coriolis effects (e.g., see eqn. (2.81) in the work of Groves (2013)). Then, vertical velocity $v^n_{eb,U}$ and altitude h_b can be assessed by successive numerical integrations (Savage, 2000).

It is well-known that such a solution for the vertical channel, i.e. altitude and vertical velocity, is inherently unstable (Siouris, 1993; Savage, 2000; Groves, 2013). A pre-existing positive altitude error δh_b leads to an underestimated local gravity, thereby a virtual upward vertical acceleration arises. Neglecting cross-coupling between the horizontal and vertical channels to solve independently as a function of initial conditions and input forces, this behavior can be approximately modeled as:

$$\delta\ddot{h}_b(t) \approx \frac{2g}{R_e}\delta h_b(t), \tag{1}$$

where g is the acceleration due to local gravity and R_e is the Earth radius at the vehicle location. Note that $2g/R_e = 2\omega_s^2$, where ω_s is the so-called Schuler frequency (Groves, 2013, Sec. 5.7.2).

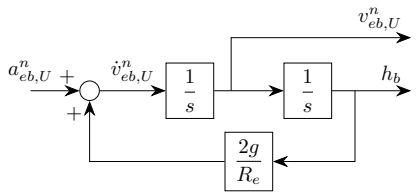

Figure 1. Block diagram for the simplified INS vertical channel algorithm

A block diagram for the simplified pure INS vertical channel described in eqn. (1) is depicted in Figure 1. The positive feedback causes the output to be unstable (Siouris, 1993, Sec. 4.5). The transfer function:

$$T_{zw}(s) = \begin{bmatrix} \dfrac{s}{s^2 - \dfrac{2g}{R_e}} & \dfrac{1}{s^2 - \dfrac{2g}{R_e}} \end{bmatrix}^T, \tag{2}$$

from $w \triangleq [a^n_{eb,U}]$ to $z \triangleq [v^n_{eb,U}\ h_b]^T$ that is associated with the INS vertical channel is unstable, with poles at $s = \pm\sqrt{2g/R_e}$. For instance, assuming zero initial conditions, this leads to an altitude error time function:

$$\delta h_b(t) = \sqrt{\frac{R_e}{2g}}\sinh\left(\sqrt{\frac{2g}{R_e}}t\right). \tag{3}$$

When $t \geq \sqrt{R_e/2g}$, the solution starts to grow exponentially and generates unacceptably large vertical navigation errors. Assuming, e.g., a vehicle at the equator, $R_e = 6378.137$ [km] and $g = 9.78$ [m/s^2], we conclude that for $t > 9.52$ [min], a pure INS solution exceeds accuracy requirements. For that reason, INS are only suited to long-term vertical navigation when it is aided by another sensor.

2.2 Barometer-aided solution

A barometric altimeter, hereinafter referred to as a barometer, is a device that measures the ambient air pressure p_B to indirectly determine the altitude, generally via a standard atmospheric model (Blanchard, 1971),

$$h_B = \frac{T_{\text{ref}}}{k_T}\left[\left(\frac{p_B}{p_{\text{ref}}}\right)^{-\frac{Rk_T}{g_0}} - 1\right] + h_{\text{ref}}, \tag{4}$$

where p_{ref} and T_{ref} are the reference pressure and temperature, h_{ref} is the geodetic altitude at which they are measured, $R = 287.1$ [J/kg K] is the gas constant, $k_T = 6.5 \times 10^{-3}$ [K/m] is the atmospheric temperature gradient, and $g_0 = 9.80665$ [m/s^2] is the standard acceleration due to gravity.

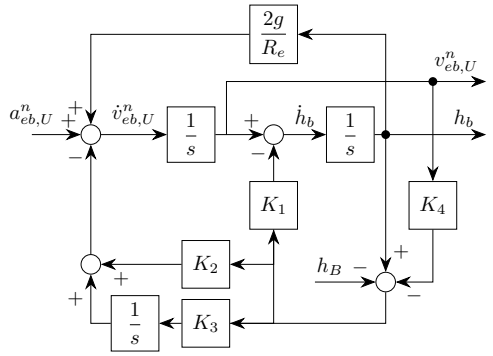

Figure 2. Third-order vertical channel mechanization with four gains

Baro-inertial fusion is traditionally employed to provide stable vertical solutions. Figure 2 depicts the 3rd-order mechanization with four gains. This multi-loop interconnection for vertical channel damping may be preferred over solutions based on Kalman filtering since it is easier to implement and understand. Even simpler interconnections can be obtained by setting K_3 or K_4 to zero.

A major performance disadvantage of the 2nd-order loop, i.e. when $K_3 = K_4 = 0$, is that it cannot avoid steady-state vertical channel errors. To improve performance, a 3rd-order loop is often used, in which K_3/s is incorporated as an integral control action in the attempt to make δh_b converge to δh_B in steady-state (Savage, 2000, Sec. 4.4.1.2.1). A feedforward control action, intended to compensate for barometer lagging, may be included as well by setting $K_4 \neq 0$ (Siouris, 1993, Sec. 4.5.3).

Given the previous recap, the problem under investigation is stated as follows:

Problem 1. Find a suitable set of gains $K \in \mathbb{R}^4$ for the 3rd-order vertical channel mechanization, such that the closed-loop system is stable and the magnitudes of the gains are, as analyzed by Savage (2000) in Sec. 4.4.1.2.1:

(a) large enough to adequately bound low-frequency signals due to accelerometer errors; and
(b) small enough to dampen high-frequency signals due to barometer errors.

Therefore, suitable gain selection is a trade-off between objectives (a) and (b) on Problem 1. Such a task relies on the design engineer's skill and experience, hence a trial-and-error method has been historically adopted. In this regard, Vieira et al. (2020) investigated the performance of various empirical tunings suggested in the literature and concluded that the most reliable is the one proposed by Savage (2000), which is able to damp barometer noise although performance is limited by its sensitivity to vehicle dynamics. A first step into optimization tuning was given by Vieira and Silva (2023) who studied LQR and performance indices minimization. In that study, the LQR approach proved to be more reliable and was able to outperform empirical tuning for different vehicle dynamics, being however, more sensitive to barometer noise. Ideally, one wants both, i.e. to properly track the barometer input while attenuating its noise.

To alleviate trial-and-error inconveniences, while seeking better performance than the ones provided by the aforementioned methods, an optimization-based procedure is proposed next.

3. OPTIMIZATION APPROACH

Consider the following mathematical optimization problem, also called optimization program:

$$\begin{aligned} &\underset{x}{\text{minimize}} \quad f(x) \\ &\text{subject to } g_i(x) \leq b_i, \quad i = 1, \ldots, m, \end{aligned} \tag{5}$$

where $x \in \mathbb{R}^n$ is the optimization variable, $f(x) : \mathbb{R}^n \to \mathbb{R}$ is the objective function and $g_i : \mathbb{R}^n \to \mathbb{R}$ are constraint functions bounded by b_i. According to Boyd and Vandenberghe (2004), program (5) deals with finding the optimal solution $x^\star$ of a given problem, i.e. the one with the smallest possible objective value among all solutions that satisfies the constraints.

When the objective function is a vector, i.e. $f(x) : \mathbb{R}^n \to \mathbb{R}^k$, (5) is called a multi-objective problem. In that case, if two solutions x and y are both feasible, x dominates y if

$$f_j(x) \leq f_j(y), \quad j = 1, \ldots, q, \tag{6}$$

and $f_k(x) < f_k(y)$, for at least one k. All points that are not dominated by any other member of the set are called Pareto-optimal, and they constitute the so-called Pareto front (Deb, 2015).

There are several classes of optimization problems and different techniques to effectively solve them. The proposed optimization method to solve Problem 1 and the analytical tools to compare the results, are discussed next.

3.1 Analytical tools

Many controller design goals can be expressed in terms of the size of signals, such as norms and statistical measures (Boyd and Barratt, 1991, Chap. 4). In this subsection, we enumerate those that will serve as metrics to describe and compare the results of the experiments.

In this work, we are interested in analyzing sampled signals, represented by a finite data set $y = \{y_1, \ldots, y_N\}$, then statistical metrics such as Mean, Average Absolute (AA), Root Mean Square (RMS), Mean Absolute Deviation (MAD) and Standard Deviation (SD), also denoted $\sigma(y)$, and signal L_p-norms These metrics will be used for three main purposes:

(a) to define an objective function;
(b) to select automatically a single solution over the Pareto front; or,
(c) to evaluate the procedure.

Throughout the work, each metric will be assigned for at least one purpose. Item (c) will be considered only in Section 4, whereas items (a) and (b) will be discussed in Subsection 3.3. Note that, performance index minimization using Integral of the Absolute Error (IAE), Integral of the Squared Error (ISE), Integral of Time multiplied by

Absolute Error (ITAE) and Integral of Time multiplied by Squared Error (ISAE) was already studied by Vieira and Silva (2023). It performed worse than the LQR approach, thus such indices will not be taken into account here.

3.2 Metaheuristic

Metaheuristic algorithms are designed to solve complex optimization problems (Bianchi et al., 2008). Such algorithms are intended to find a nearly optimal solution in a reasonable computation time; therefore, their solution is suboptimal rather than optimal. Evolutionary computation uses methods inspired by Darwinian evolution to explore the search space. This article specifically focuses on Genetic Algorithms (GA), which have been first proposed by Holland (1975). In this context, the n-dimensional optimization variable is called an individual, which carries a genotype to be mutated (varied) and based on evaluation by a fitness function. Evolution is carried over generations, wherein each generation includes a set of individuals evaluated relative to each other. A first population includes n_{pop} random individuals. Subsequently, at each generation, genetic operations (i.e., selection, recombination, and mutation) create a new population for the next generation. When the maximum number of generations n_{gen} is reached, the fittest individual is selected.

As stated by Judson (2009), selection drives the population towards convergence, while recombination and mutation drive it towards more diverse solutions. The combined genetic operations are designed to achieve a trade-off that prevents the loss of good solutions, while searching for better ones, and prevents the optimization from getting stuck in local minima. Selection of the hyperparameters n_{pop} and n_{gen} directly impacts the ability of the algorithm to explore the search area and its computation time, and is problem-dependent (Judson, 2009). For instance, the total CPU time in an optimization run

$$t_{\text{CPU}} \propto (n_{\text{pop}} \times n_{\text{gen}} \times t_f), \tag{7}$$

where t_f corresponds to the time required to evaluate the fitness function of an individual.

As indicated in Section 3.1, there are several functions that can be used for fitness scoring purposes. The approach adopted in this paper is described next.

3.3 Evolutionary tuning

We start by representing the mapping from $w \triangleq [a^n_{eb,U}\ h_B]^T$ to $z \triangleq [v^n_{eb,U}\ h_b]^T$ for the 3rd-order mechanization depicted in Figure 2 by state-space equations of the form:

$$T_{zw}(s,K) = \left[\begin{array}{c|c} A(K) & B(K) \\ \hline C(K) & D(K) \end{array}\right], \tag{8}$$

where $K \in \mathbb{R}^4$ represents a vector of tunable gains. We also assume that the design engineer has experimental data sets available that represent the final application well enough for tuning purposes.

Each individual is a specific value for the vector K. Individuals are only included in a population if: (1) they result in a stable closed-loop system; and, (2) the magnitude of each element of K is bounded by a given positive real value k that is selected by the design engineer. Constraint (1) is evaluated by checking if all the eigenvalues of the state-space A-matrix in (8), denoted as $\lambda_i\left(A(K)\right)$, are in the open left-half plane (Skogestad and Postlethwaite, 2005).

Next, a fitness function must be defined to evaluate the individuals. For that purpose, we choose the standard deviation of the error response over time of a given altitude profile for a predefined vector of tuned gains $\sigma(\delta h_b(K))$. Thus, the goal is to solve the vertical channel problem via the following optimization program:

$$\begin{aligned} \underset{K}{\text{minimize}} \quad & \sigma(\delta h_b(K)) \\ \text{subject to} \quad & \max_i \operatorname{Re}\left\{\lambda_i\left(A(K)\right)\right\} < 0, \\ & |K_j| \le k, \quad k > 0, \quad \forall j \in \{1,2,3,4\}. \end{aligned} \tag{9}$$

To solve program (9), a random initial population is generated based on initialization parameters. Then, stability is checked for each individual: if it provides an unstable loop the score is set to ∞; otherwise a real data set corresponding to a sequence of maneuvers, e.g. in an aircraft or in a car, is used to generate a baro-inertial navigation system output profile and to compute its respective score. Based on the population scores, evolutionary computation is carried out. The overall procedure is illustrated in the form of a flowchart in Figure 3.

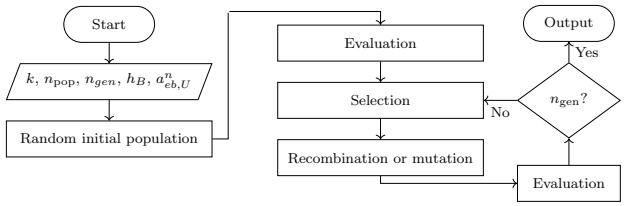

Figure 3. Genetic algorithm procedure flowchart

Alternatively, one can think in a multi-objective approach, which also takes into account the SD of the error response over time of the vertical velocity profile. In that case, the problem is tackled with the following program:

$$\begin{aligned} \underset{K}{\text{minimize}} \quad & \left(\sigma(\delta h_b(K)),\, \sigma(\delta v^n_{eb,U}(K))\right) \\ \text{subject to} \quad & \max_i \operatorname{Re}\left\{\lambda_i\left(A(K)\right)\right\} < 0, \\ & |K_j| \le k, \quad k > 0, \quad \forall j \in \{1,2,3,4\}. \end{aligned} \tag{10}$$

In this work, the routine GA is adopted to solve (9), while GAMULTIOBJ, which is a variant of the NSGA-II method proposed by Deb et al. (2002), is used to search for the Pareto front on the problem (10). Both solvers are implemented in MATLAB.

In this regard, following Deb (2015), evolutionary multi-objective optimization are similar to *a posteriori* decision-making methods. Thus, the procedure comprises two steps:

(1) multiple Pareto-optimal solutions are attempted to be found in a single run of the program (10); then,
(2) higher-level analysis is used by the design engineer to choose one of the trade-off points obtained.

It is noteworthy that choosing one solution over the Pareto front is nontrivial, as each nondominant solution represents a different trade-off among the objectives. One may advocate the use of *a priori* approaches instead, but without knowing good trade-off regions beforehand may encourage the design engineer to settle for a solution which, although optimal, may not be a good compromise solution.

After some experiments, we adopted the method suggested by Padhye and Deb (2011) and de la Fuente et al. (2018), which uses the L_2-norm of the normalized objectives to select a single solution from the Pareto front. In other words, the objectives are rescaled in the range $[0, 1]$ as follows:

$$\hat{\sigma}(\delta h_b)_i^{\text{po}} = \frac{\sigma(\delta h_b)_i^{\text{po}} - \min_i \sigma(\delta h_b)_i^{\text{po}}}{\max_i \sigma(\delta h_b)_i^{\text{po}} - \min_i \sigma(\delta h_b)_i^{\text{po}}}, \tag{11}$$

and

$$\hat{\sigma}(\delta v^n_{eb,U})_i^{\text{po}} = \frac{\sigma(\delta v^n_{eb,U})_i^{\text{po}} - \min_i \sigma(\delta v^n_{eb,U})_i^{\text{po}}}{\max_i \sigma(\delta v^n_{eb,U})_i^{\text{po}} - \min_i \sigma(\delta v^n_{eb,U})_i^{\text{po}}}. \tag{12}$$

Then, a single solution is selected as

$$K^\star \triangleq \arg\min_{K \in K^{\text{po}}} \left\| \begin{bmatrix} \hat{\sigma}(\delta h_b(K))^{\text{po}} \\ \hat{\sigma}(\delta v^n_{eb,U}(K))^{\text{po}} \end{bmatrix} \right\|_2. \tag{13}$$

4. RESULTS

To validate the mechanization tuning method proposed in Section 3.3, as well as to compare its performance with other tunings found in the literature, we conducted experimental tests with real data sets, corresponding to the measurements collected with Xsens (2023a,b,c) modules for different vehicles dynamics.

The optimization procedure described in Section 3.3 was performed both with a small airplane and a car test-drive data sets, $k = 5$, $n_{\text{pop}} = 100$, and $n_{\text{gen}} = 10$ in the single objective approach. The multi-objective instance, in turn, was performed with $n_{\text{gen}} = 30$.

Table 1. Mechanization gains

Tuning	K_1	K_2	K_3	K_4
Savage	0.30	0.03	1.00×10^{-3}	0.00
LQR	2.41	2.41	1.00	0.00
$\text{GA}_\text{f}^\text{so}$	3.12	1.36	0.07	0.80
$\text{GA}_\text{f}^\text{mo}$	4.09	1.18	0.36	0.59
$\text{GA}_\text{d}^\text{so}$	4.94	0.85	0.32	−0.69
$\text{GA}_\text{d}^\text{mo}$	4.72	0.58	6.16×10^{-3}	−1.08

Table 1 summarizes the final tuning of each analyzed mechanization, where $\text{GA}_\text{f}^\text{so}$ and $\text{GA}_\text{f}^\text{mo}$ denotes the single and multi-objective approaches for the flight test respectively, while $\text{GA}_\text{d}^\text{so}$ and $\text{GA}_\text{d}^\text{mo}$ denotes the same approaches for the car test-drive. Along with the GA-based tunings, the empirical tuning suggested by Savage (2000) and the LQR tuning proposed by Vieira and Silva (2023) were also investigated.

The method by Vieira and Silva (2023) relies on an under-determined system of equations, based on which the authors arbitrarily assigned K_4 as zero. The GA approach, in turn, does not need to take this additional constraint into account, (see the formulation of programs (9) and (10) for details), as each gain is assigned during the GA optimization procedure.

4.1 Flight test

The first experiment employed a real data set collected with MTi-G-710 modules, manufactured by Xsens (2023c), during an aircraft flight test conducted at Nordhorn-Lingen Airport, Germany, on January 23, 2018. Both raw data from the sensors and ground-truth solution from the modules were collected and stored for post-processing (Xsens, 2018). As done by Vieira and Silva (2023), the flight was divided into three different segments, representing particular vehicle dynamics. For tuning purposes, we only used the 1st segment of flight. To establish reliable ground-truth values for the aircraft vertical channel, a post-processed solution was adopted, which relies on additional auxiliary sensors such as multi-constellation GNSS receivers, magnetometers, and sophisticated sensory fusion algorithms.

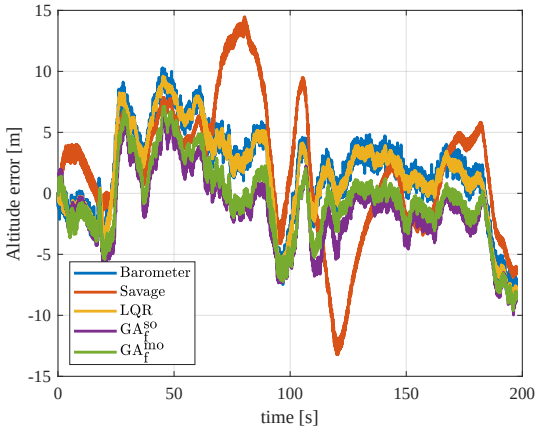

Figure 4. Altitude error during the first flight segment

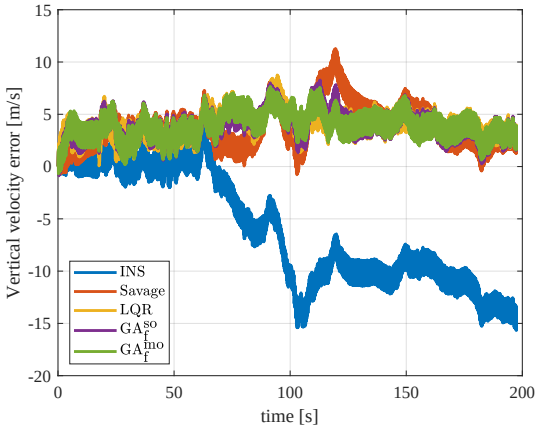

Figure 5. Vertical velocity error during the first flight segment

Table 2. Metrics for the first flight segment

Metric		Tuning				
		Baro/INS	Savage	LQR	$\text{GA}_\text{f}^\text{so}$	$\text{GA}_\text{f}^\text{mo}$
Altitude [m]	RMS	4.20	5.93	4.17	3.30	3.22
	Peak	10.25	14.47	9.61	9.97	9.61
	Mean	1.85	2.12	1.77	−1.20	−0.45
	AA	3.46	4.77	3.41	2.58	2.40
	SD	3.77	5.54	3.78	3.08	3.19
	MAD	2.91	4.34	2.91	2.33	2.36
Vert. vel. [m/s]	RMS	8.12	4.31	4.13	4.13	4.13
	Peak	15.67	11.26	8.76	8.28	7.66
	Mean	−6.03	3.81	3.93	3.92	3.92
	AA	6.49	3.82	3.93	3.91	3.93
	SD	5.44	2.01	1.29	1.34	1.28
	MAD	5.01	1.58	1.02	1.06	1.02
Ranking		5	4	2	2	1

Figure 4 depicts the altitude error profiles during the first segment of flight generated by the mechanizations summarized in Table 2. It additionally depicts the reference vertical error, i.e. the pure barometer output error δh_B.

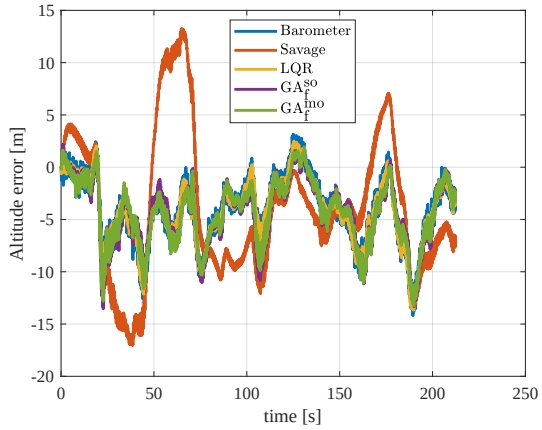

Figure 6. Altitude error response during the third flight segment

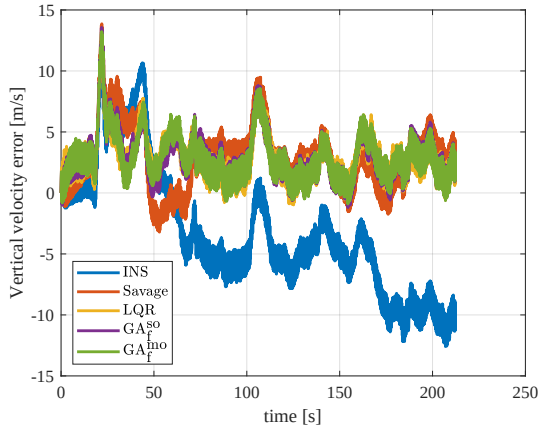

Figure 7. Vertical velocity error response during the third flight segment

Table 3. Metrics for the third flight segment

Metric		Tuning				
		Baro/INS	Savage	LQR	GA_f^{so}	GA_f^{mo}
Altitude [m]	RMS	5.16	7.85	5.19	5.25	5.20
	Peak	14.20	17.04	13.67	13.55	13.27
	Mean	−4.04	−3.76	−4.09	−4.25	−4.21
	AA	4.23	6.73	4.27	4.34	4.33
	SD	3.21	6.89	3.19	3.08	3.05
	MAD	2.61	5.50	2.60	2.55	2.41
Vert. vel. [m/s]	RMS	6.13	3.88	3.48	3.51	3.50
	Peak	12.59	13.87	13.03	13.55	13.21
	Mean	−3.15	2.85	2.93	2.92	2.93
	AA	5.28	3.12	2.94	2.94	2.94
	SD	5.26	2.63	1.87	1.95	1.92
	MAD	4.21	2.00	1.40	1.46	1.46
Ranking		4	5	1	3	1

Figure 5 depicts the vertical velocity errors, for the same segment using each mechanization summarized in Table 2 and the pure INS output (i.e., $K = 0$). Table 2 provides a collection of the metrics discussed in Section 3.1, which were computed from the signals shown in Figures 4 and 5. For each metric, the tuning that performed the best is highlighted in green and the one that performed the worst is highlighted in red.

As can be readily verified, the GA_f^{mo} tuning achieved the best performance in 8 out of 12 of the considered metrics and was very close to the best in the remaining 4. The tuning by Savage (2000), in turn, performed poorly w.r.t. altitude errors and the one by LQR (Vieira and Silva, 2023) was never the worst or single best. Such an outperformance by the GA approaches was expected since the optimization used the same data set as the evaluation.

Reasonably, one may inquire about the performance of the proposed tuning with a different data set. Hence, the third fight segment was considered for further investigation of the proposed tuning method. Note that this flight segment was carefully chosen because its similarity, in terms of dynamics, to the first segment.

Figures 6 and 7 depict the altitude and vertical velocity errors, respectively, for the third flight segment. Its metrics are summarized in Table 3. It is noteworthy that the GA_f^{mo} tuning still performs best w.r.t. altitude errors and ties overall with the LQR tuning (Vieira and Silva, 2023), despite being optimized for a different data set. Note also that, in both scenarios, the multi-objective approach improves the overall result achieved when only one objective is used in the optimization procedure, at the cost, however, of extra computational effort.

4.2 Car test-drive

The second experiment employed two data sets collected with MTi-680G and MTi-7 modules (Xsens, 2023a,b), respectively, during a car test-drives conducted at Lavras, Minas Gerais, on February 27, 2023. As in the previous experiment, both raw data from the sensors and ground-truth solution from the modules were collected and stored for post-processing and a single data set was used for optimization purposes, namely, the MTi-7 data set. The aim of this experiment was to evaluate the performance of the previously optimized mechanizations (i.e., GA_f^{so} and GA_f^{mo}) under different data sets, dynamics, and sensors.

Figures 8 and 9, depict the altitude and vertical velocity error profiles while Table 4 summarizes the metrics for the MTi-7 experiment. Again, the pure barometer or INS outputs are also displayed for comparison purposes. Comparing the metrics in Tables 2 and 3 with those in Table 4, performance degradation is noticeable for all tunings. In particular, the GA_f^{so} and GA_f^{mo} tunings for aircraft are used in this driving data set (referring to a completely different vehicular dynamic). Nevertheless, the multi-objective procedure was able to provide better sub-optimal solutions when tuned with the appropriate data set, i.e., GA_d^{mo}. Such tuning achieved the best performance in 8 out of 12 metrics while being reasonably close to the best in the remaining 4.

Based on the aforementioned results, one additional question seems important: does the proposed tuning method degrade only for different vehicle dynamics or also for different sensor grades? To answer that, we also examined the MTi-680G data set collected for the same car trajectory as in the MTi-7 test. In agreement with the previous analysis methodology, the altitude and vertical velocity error profiles are depicted in Figures 10 and 11, respectively, while Table 5 summarizes the metrics for the MTi-680G experiment. Remarkably, the GA_d^{mo} tuning still performed best overall, despite being optimized using a data set collected with a different module (MTi-7), for the same car trajectory though, depicting the lowest value in 5 out of 12 metrics. These results imply that such method is robust w.r.t. sensor/data change, provided that the vehicle

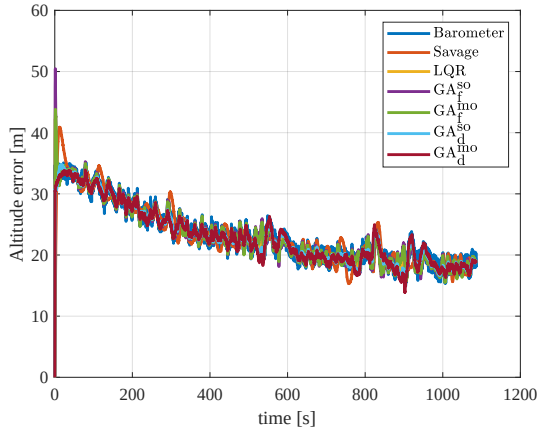

Figure 8. Altitude error response for the MTi-7 experiment

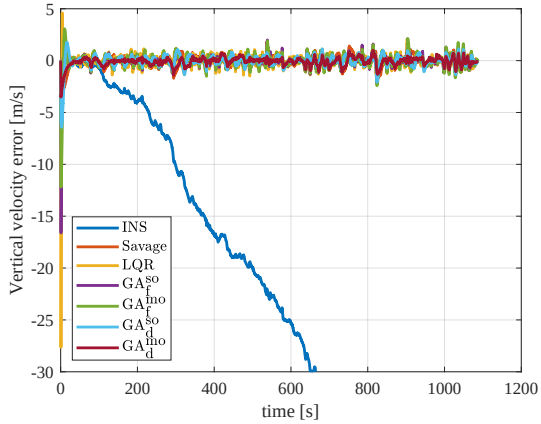

Figure 9. Vertical velocity error response for the MTi-7 experiment

Table 4. Metrics for the MTi-7 experiment

Metric		Tuning						
		Baro/INS	Savage	LQR	GA_f^{so}	GA_f^{mo}	GA_d^{so}	GA_d^{mo}
Altitude [m]	RMS	23.74	23.79	23.63	23.69	23.67	23.60	23.53
	Peak	35.15	40.92	42.26	50.46	43.83	34.79	33.92
	Mean	27.32	27.34	27.32	27.35	27.29	27.34	27.16
	AA	27.32	27.34	27.32	27.35	27.29	27.34	27.16
	SD	4.69	5.11	4.79	4.93	4.89	4.74	4.75
	MAD	3.82	4.06	3.90	3.96	3.95	3.88	3.89
Vert. vel. [m/s]	RMS	33.97	0.54	1.04	0.77	0.86	0.64	0.42
	Peak	69.12	2.74	27.64	16.61	12.19	6.43	3.52
	Mean	−26.85	−0.06	−0.03	−0.04	−0.03	−0.03	−0.10
	AA	26.85	0.38	0.38	0.35	0.47	0.38	0.28
	SD	20.80	0.53	1.04	0.77	0.86	0.64	0.41
	MAD	17.91	0.38	0.38	0.35	0.47	0.39	0.28
Ranking		7	5	2	5	2	2	1

dynamics used in the optimization are similar to the one being assessed. Such a feature may be relevant for vehicles subject to systematically repeated maneuvers.

5. CONCLUSION

This study revisited the problem of vertical channel damping of barometer-aided INS via 3rd-order control loops. Evolutionary optimization procedures have been studied to tune such mechanizations. As verified by means of experimental results, the multi-objective optimization using GA outperforms the gains tuned by other mechanisms. The method proved to be reliable for different data sets, collected by different sensors or during slightly different maneuvers. In other words, provided that the vehicle

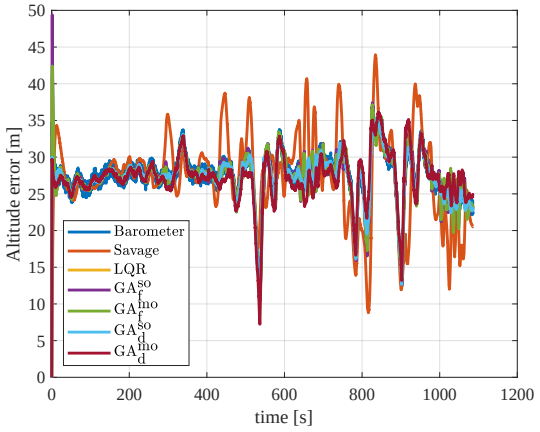

Figure 10. Altitude error response for the MTi-680G experiment

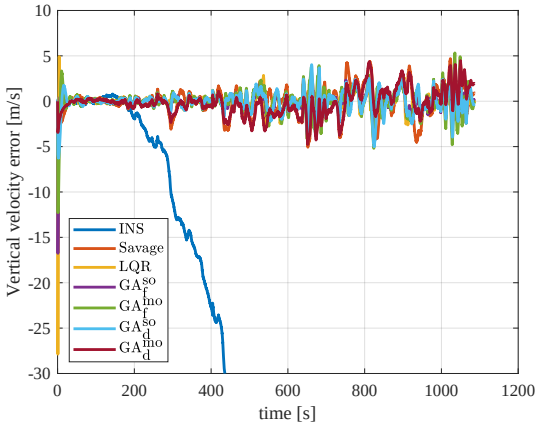

Figure 11. Vertical velocity error response for the MTi-680G experiment

Table 5. Metrics for the MTi-680G experiment

Metric		Tuning						
		Baro/INS	Savage	LQR	GA_f^{so}	GA_f^{mo}	GA_d^{so}	GA_d^{mo}
Altitude [m]	RMS	27.51	27.94	27.50	27.57	27.56	27.47	27.36
	Peak	36.08	43.95	40.94	49.40	42.41	35.54	36.15
	Mean	27.32	27.34	27.32	27.35	27.34	27.29	27.16
	AA	27.32	27.34	27.32	27.35	27.34	27.29	27.16
	SD	3.20	5.80	3.22	3.47	3.44	3.15	3.29
	MAD	2.11	4.22	2.09	2.26	2.27	2.06	2.04
Vert. vel. [m/s]	RMS	162.05	1.60	1.21	1.12	1.39	1.18	1.43
	Peak	304.95	5.07	27.87	16.75	12.27	6.28	4.74
	Mean	−115.40	−0.05	−0.04	−0.04	−0.04	−0.04	−0.17
	AA	115.46	1.15	0.51	0.65	0.89	0.79	1.03
	SD	113.78	1.60	1.21	1.12	1.39	1.18	1.42
	MAD	103.67	1.15	0.52	0.65	0.89	0.79	1.01
Ranking		7	6	2	5	4	2	1

dynamics are similar enough to those used in the optimization procedure, the proposed technique can achieve better performance when compared to other state-of-the-art techniques. As a suggestion for future works, there is the use of adaptive and robust control techniques for the baro-INS vertical channel mechanization tuning. Also the study of systematic methods for robustness assessment of such tunings.

REFERENCES

Bekir, E. (2007). *Introduction to Modern Navigation Systems*. World Scientific Publishing Company.

Ben, Y., Cui, W., and Li, Q. (2023). A new gains-selection method of depth gauge aided vertical channel

for underwater vehicles. *Measurement*, 214, 112761. doi:10.1016/j.measurement.2023.112761.

Bianchi, L., Dorigo, M., Gambardella, L.M., and Gutjahr, W.J. (2008). A survey on metaheuristics for stochastic combinatorial optimization. *Nat. Comput.*, 8, 239–287. doi:10.1007/s11047-008-9098-4.

Blanchard, R. (1971). A new algorithm for computing inertial altitude and vertical velocity. *IEEE T. Aero. Elec. Sys.*, AES-7(6), 1143–1146. doi:10.1109/TAES.1971.310216.

Boyd, S. and Barratt, C. (1991). *Linear Controller Design: Limits of Performance*. Prentice Hall.

Boyd, S. and Vandenberghe, L. (2004). *Convex Optimization*. Cambridge University Press.

de la Fuente, D., Vega-Rodríguez, M.A., and Pérez, C.J. (2018). Automatic selection of a single solution from the Pareto front to identify key players in social networks. *Knowl.-Based Syst.*, 160, 228–236. doi:10.1016/j.knosys.2018.07.018.

de Morais, G.A.P., Marcos, L.B., Barbosa, F.M., Barbosa, B.H., Terra, M.H., and Grassi, V. (2022). Robust path-following control design of heavy vehicles based on multiobjective evolutionary optimization. *Expert Syst. Appl.*, 192, 116304. doi:10.1016/j.eswa.2021.116304.

de Silva, C.W. (2009). Intelligent control. In R.A. Meyers (ed.), *Encyclopedia of Complexity and Systems Science*, 4868–4891. Springer, New York, NY. doi:10.1007/978-0-387-30440-3_288.

Deb, K., Pratap, A., Agarwal, S., and Meyarivan, T. (2002). A fast and elitist multiobjective genetic algorithm: NSGA-II. *IEEE T. Evolut. Comput.*, 6(2), 182–197. doi:10.1109/4235.996017.

Deb, K. (2015). Multi-objective evolutionary algorithms. In J. Kacprzyk and W. Pedrycz (eds.), *Springer Handbook of Computational Intelligence*, 995–1015. Springer, Berlin, Heidelberg. doi:10.1007/978-3-662-43505-2_49.

Dracopoulos, D.C. (1997). Genetic algorithms and genetic programming for control. In D. Dasgupta and Z. Michalewicz (eds.), *Evolutionary Algorithms in Engineering Applications*, 329–343. Springer, Berlin, Heidelberg. doi:10.1007/978-3-662-03423-1_19.

Farrell, J.A. (2008). *Aided Navigation: GPS with High Rate Sensors*. McGraw-Hill, Inc.

Farrell, J.A. and Wendel, J. (2017). GNSS/INS integration. In P.J. Teunissen and O. Montenbruck (eds.), *Springer Handbook of Global Navigation Satellite Systems*, 811–840. Springer, Cham. doi:10.1007/978-3-319-42928-1_28.

Gallo, E. and Barrientos, A. (2022). Reduction of GNSS-denied inertial navigation errors for fixed wing autonomous unmanned air vehicles. *Aerosp. Sci. Technol.*, 120, 107237. doi:10.1016/j.ast.2021.107237.

Goldberg, D.E. (1989). *Genetic Algorithms in Search, Optimization, and Machine Learning*. Addison-Wesley Professional, 1st edition.

Groves, P.D. (2013). *Principles of GNSS, Inertial, and Multisensor Integrated Navigation Systems*. Artech House Publishers, 2nd edition.

He, H., Jiangning, X., Feng, L., and Miao, W. (2016). Genetic algorithm based optimal compass alignment. *IET Radar, Sonar & Nav.*, 10(2), 411–416. doi:10.1049/iet-rsn.2015.0314.

Holland, J.H. (1975). *Adaptation in Natural and Artificial Systems*. The MIT Press.

Judson, R.S. (2009). Genetic algorithms. In C.A. Floudas and P.M. Pardalos (eds.), *Encyclopedia of Optimization*, 1254–1257. Springer, Boston, MA. doi:10.1007/978-0-387-74759-0_218.

Kirk, D.E. (2004). *Optimal Control Theory: An Introduction*. Dover Publications.

Ogata, K. (2010). *Modern Control Engineering*. Prentice Hall, 5th edition.

Padhye, N. and Deb, K. (2011). Multi-objective optimisation and multi-criteria decision making for FDM using evolutionary approaches. In L. Wang, A.H.C. Ng, and K. Deb (eds.), *Multi-objective Evolutionary Optimisation for Product Design and Manufacturing*, 219–247. Springer, London. doi:10.1007/978-0-85729-652-8_7.

Rogers, R.M. (2007). *Applied Mathematics in Integrated Navigation Systems*. AIAA, 3rd edition.

Savage, P.G. (2000). *Strapdown Analytics*, volume 1. Strapdown Associates, 1st edition.

Silva, F.O. and Vieira, L.A. (2022). Optimizing the gains of baro-inertial vertical channel mechanizations. In *Proc. 31st Int. Symp. Industrial Electronics*, 582–588. IEEE. doi:10.1109/ISIE51582.2022.9831633.

Siouris, G. (1993). *Aerospace Avionics Systems: A Modern Synthesis*. Academic Press.

Skogestad, S. and Postlethwaite, I. (2005). *Multivariable Feedback Control: Analysis and Design*. Wiley, 2nd edition.

Titterton, D. and Weston, J. (2005). *Strapdown Inertial Navigation Technology*. The Institution of Engineering and Technology, 2nd edition.

Vieira, L.A. and Silva, F.O. (2023). Vertical channel stabilization of barometer-aided inertial navigation systems by optimal control. *Asian J. Control*. doi:10.1002/asjc.3058.

Vieira, L.A., Silva, F.O., Menezes Filho, R.P., and Paiva, L.P.S. (2020). Performance indices-based tuning for barometer-aided inertial navigation systems. In *Latin American Robotics Symp.*, 1–6. IEEE. doi:10.1109/LARS/SBR/WRE51543.2020.9307162.

Wang, Q., Spronck, P., and Tracht, R. (2003). An overview of genetic algorithms applied to control engineering problems. In *Proc. of the 2003 ICMLC*, volume 3, 1651–1656. IEEE. doi:10.1109/ICMLC.2003.1259761.

Widnall, W.S. and Sinha, P.K. (1980). Optimizing the gains of the baro-inertial vertical channel. *J. Guid. Control*, 3(2), 172–178. doi:10.2514/3.55966.

Xsens (2018). Flying high with the Xsens test team. URL `https://www.movella.com/resources/blog/flying-high-with-the-xsens-test-team`.

Xsens (2023a). MTi-680G RTK GNSS/INS. URL `https://www.movella.com/products/sensor-modules/xsens-mti-680g-rtk-gnss-ins`.

Xsens (2023b). MTi-7 GNSS/INS. URL `https://www.movella.com/products/sensor-modules/xsens-mti-7-gnss-ins`.

Xsens (2023c). MTi-G-710 GNSS/INS. URL `https://www.movella.com/products/sensor-modules/xsens-mti-g-710-gnss-ins`.